bioRxiv preprint doi: https://doi.org/10.1101/502922; this version posted December 21, 2018. The copyright holder for this preprint (which was not certified by peer review) is the author/funder, who has granted bioRxiv a license to display the preprint in perpetuity. It is made available under aCC-BY-NC-ND 4.0 International license.

1 **Pre-Clinical Blocking of PD-L1 molecule, which expression is down regulated by NF-κB,**
2 **JAK1/JAK2 and BTK inhibitors, induces regression of activated B-cell lymphoma.**

3 Christelle Vincent-Fabert[1], Lilian Roland[1], Ursula Zimber-Strobl[4], Jean Feuillard[1], Nathalie
4 Faumont[1]

5 [1]CNRS-UMR 7276 CRIBL, University of Limoges, and Hematology Laboratory of
6 Dupuytren Hospital University Center (CHU) of Limoges; France; and [4]Research Unit Gene
7 Vectors, Helmholtz Center Munich, German Research Center for Environmental Health
8 GmbH, Munich, Germany.

9 **Running title**: PD-L1 targeting of activated B-cell lymphomas

10 **Corresponding Author:** Nathalie Faumont; CNRS-UMR 7276 CRIBL "Contrôle de la
11 Réponse Immune B et Lymphoproliférations", CBRS "Centre de Biologie et de Recherche en
12 Santé", Dupuytren Hospital University Center, University of Limoges, Hematology
13 Laboratory of Dupuytren CHU, 2 rue du Docteur Marcland, 87025 Limoges, France. ph: +33
14 (0)5 19 56 42 21; fax: +33 (0)5 55 43 58 97; and email: nathalie.faumont@unilim.fr.

15 **Conflict of Interest:** The authors declare no conflict of interest.

16 **Keywords:** Indolent B-cell lymphoma, PD-L1, Immune surveillance

17

18 **Financial support:** The group of J Feuillard is supported by grants from the Ligue National
19 contre le Cancer (Equipe Labellisée Ligue), the Institut National du Cancer (INCa), the
20 Comité Orientation Recherche Cancer (CORC), the Limousin Region and the Haute Vienne
21 and Corrèze committees of the Ligue Nationale Contre le Cancer and by the Lyons Club of
22 Corrèze. U Zimber-Strobl was supported by the German Research Foundation (SFB 1243,
23 TP-A13).

24
25 **Word count in text:** 1357
26 **Total number of Figures:** 4
27 **Supplementary Tables:** 3
28 **References:** 15

bioRxiv preprint doi: https://doi.org/10.1101/502922; this version posted December 21, 2018. The copyright holder for this preprint (which was not certified by peer review) is the author/funder, who has granted bioRxiv a license to display the preprint in perpetuity. It is made available under aCC-BY-NC-ND 4.0 International license.

29 **Abstract**

30 Escape from immune control must be important in the natural course of B-cell lymphomas,
31 especially for those with activation of NF-κB. The pre-clinical L.CD40 transgenic mouse
32 model is characterized by B-cell specific CD40 signaling responsible for NF-κB continuous
33 activation with a spleen monoclonal B-cell tumor after one year in 60% of cases. L.CD40
34 tumors B-cells expressed high levels of PD-L1. This expression was dependent on activation
35 of either NF-κB, JAK1/JAK2 or BTK pathways since ex vivo treatment with the inhibitory
36 molecules PHA-408, ruxolitinib and ibrutinib led to decrease of its expression. Treatment of
37 L.CD40 lymphomatous mice with an anti-PD-L1 monoclonal antibody induced tumor
38 regression with decreased spleen content, activation and proliferation rate of B-cells as well as
39 a marked increase in T cell activation, as assessed by CD62L and CD44 expression. These
40 results highlight the interest of therapies targeting the PD-1/PD-L1 axis in activated
41 lymphomas with PD-L1 expression, with possible synergies with tyrosine kinase inhibitors.

42

bioRxiv preprint doi: https://doi.org/10.1101/502922; this version posted December 21, 2018. The copyright holder for this preprint (which was not certified by peer review) is the author/funder, who has granted bioRxiv a license to display the preprint in perpetuity. It is made available under aCC-BY-NC-ND 4.0 International license.

43 **Introduction**

44 Aberrant expression of the programmed death-ligand 1 (PD-L1, also known as B7-H1 or
45 CD274) checkpoint molecule has been reported in many cancers such as breast, lung and
46 colon tumors as well as during chronic viral infections like Epstein-Barr virus (EBV)
47 infection for example (1,2). Efficacy of immunotherapies against the PD-1/PD-L1 axis in
48 breast or colon cancers demonstrated the importance of the immune checkpoints in the control
49 of emergence and growth of tumors (2). As reviewed recently, various publications have
50 indicated that disruption of immune checkpoints is also a critical step in B-cell non-Hodgkin's
51 Lymphomas (NHL) (3). NF-κB, one of the most cited transcription factor in B-cell
52 lymphomas, is able to increase tumor cell expression of PD-L1 either directly or indirectly
53 (3). NF-κB constitutive activation is found either in aggressive diffuse large B-cell
54 lymphomas (DLBCL) with an activated phenotype (ABC-DLBCL), or in indolent B-cell
55 lymphomas such as chronic lymphocytic leukemia, Waldenström Macroglobulinemia,
56 marginal zone B-cell lymphomas (MZL) (4). Here, we wanted to explore the putative interest
57 of PDL-1 immune therapy against B-cell lymphoma with NF-κB activation. To
58 experimentally address this question, we used a transgenic mouse model which specifically
59 express in B-cells a chimeric protein composed of the transmembrane moiety of the Epstein
60 Barr Virus latent membrane protein 1 (LMP1) and the transduction tail of CD40 (L.CD40
61 protein), that results in continuous activation of NF-κB, responsible for a spleen monoclonal
62 B-cell tumor (L.CD40 B-cell lymphoma) after one year in 60% of cases (5).

63

64 **Results**

65 Our previous transcriptome studies from L.CD40 mice suggested that those tumors might
66 express high levels of CD274/PD-L1 (6). We thus analyzed the Immune Escape Gene

bioRxiv preprint doi: https://doi.org/10.1101/502922; this version posted December 21, 2018. The copyright holder for this preprint (which was not certified by peer review) is the author/funder, who has granted bioRxiv a license to display the preprint in perpetuity. It is made available under aCC-BY-NC-ND 4.0 International license.

67 Signature published by C Laurent *et al* (Supplemental Table 1) (7) from the Affymetrix
68 transcriptome (HT MG-430 PM Array, Supplemental Tables 2 and 3) of a series of six
69 L.CD40 B-cell lymphomas that were compared to their CD19_Cre littermate. As shown in
70 Figure 1A, both PD-L1 (red arrow) and PD-L2 (orange arrow) were co-clusterized with the
71 immunosuppressive interleukin 10 (IL-10, green arrow), CD80 and MCL1, being over
72 expressed. Indeed, L.CD40 lymphoma cells from 12 months old mice expressed higher levels
73 of PD-L1 than B-cells from age related CD19_Cre mice (Figure 1B).

74

75 In addition to be able to activate the classical pathway, CD40 is a strong inducer of the
76 alternative NF-κB activating pathway. CD40 constitutive activation of B-cells increases IL-10
77 expression (8). As mentioned above, IL-10 gene expression was co-clusterized with the one of
78 PD-L1 and PD-L2, being up-regulated in L.CD40 B-cell lymphoma (Figure 1A). IL-10
79 receptor signaling is mediated by the JAK1 and Tyk2 tyrosine kinase that leads to activation
80 of STAT3 transcription factor, STAT3 being a major inducer of PD-L1 gene expression (9).
81 CD40 stimulation can also augment BCR-induced B cell responses by activation of Bruton's
82 tyrosine kinase (BTK) (10), and the BCR is also able to induce the IL-10/STAT3 signaling
83 with increased expression of PD-L1 in diffuse large B-cell lymphoma (9). We thus *ex vivo*
84 treated purified L.CD40 lymphoma B-cells with the PHA-408 molecule, an inhibitor of
85 IKK2/NF-κB activation, the JAK1/JAK2 tyrosine kinase inhibitor (TKI) ruxolitinib, and the
86 BTK inhibitor ibrutinib. As shown in Figure 2, PD-L1 expression was strongly reduced 48h
87 after treatment with either PHA-408 or ruxolitinib and moderately with ibrutinib, a strong
88 indication that PD-L1 expression was under control of CD40 activation, either directly
89 through NF-κB activation or indirectly through IL-10 induction of BCR sensitization and
90 BTK activation.

bioRxiv preprint doi: https://doi.org/10.1101/502922; this version posted December 21, 2018. The copyright holder for this preprint (which was not certified by peer review) is the author/funder, who has granted bioRxiv a license to display the preprint in perpetuity. It is made available under aCC-BY-NC-ND 4.0 International license.

91

92 To address *in vivo* the role of PD-L1 in these B-cell lymphoma, L.CD40 mice were treated
93 with an antibody blocking programmed cell death protein 1 (PD-1)/PD-1 1igand 1 (PD-L1)
94 signaling for three weeks according to a methodology already described (11,12). We observed
95 a reduction of spleen size and absolute number of splenocytes in anti-PD-L1 treated L.CD40
96 mice (Figure 3A), due to decreased B-cell numbers (Figure 3B). With PD-L1 blockade, we
97 noticed a decrease in numbers of activated B-cells in L.CD40 mice (Figure 3C). This was
98 associated with a reduction in the *in vivo* proliferation rate of spleen B-cells, as assessed by
99 the decrease of *in vivo* BrdU incorporation over 18 hours (Figure 3D). Morphologically,
100 spleen lymphocytes from anti-PD-L1 treated L.CD40 mice were smaller with a more
101 condensed chromatin (Figure 3E). We then studied the impact of PD1/PD-L1 blockade in T-
102 cell compartment. Expression of T-cell activation markers CD62L and CD44 was increased
103 on both $CD4^+$ and $CD8^+$ T-cells (Figure 4A). In parallel, an increase in PD-1 expression was
104 observed on the surface of CD4 T-cells. This increase in PD-1 expression was more
105 heterogeneous on CD8 T-cells (Figure 4B).

106

107 **Discussion**

108 Expression of PD-1 and PD-L1 in B-cell lymphomas and effect of immune therapies against
109 the immune checkpoint axe has been recently reviewed (3). Expression of PD-L1 by tumor
110 cells and effect of anti-PD-1 immune therapy has been clearly demonstrated in Hodgkin's
111 lymphoma, a tumor which is constantly associated with both NF-κB and STAT3 activation. In
112 DLBCL, expression of PD-L1 is variable but participates to the gene immune escape
113 signature of ABC-DLBCLs (3,7). ABC-DLBCL are not only associated with NF-κB

bioRxiv preprint doi: https://doi.org/10.1101/502922; this version posted December 21, 2018. The copyright holder for this preprint (which was not certified by peer review) is the author/funder, who has granted bioRxiv a license to display the preprint in perpetuity. It is made available under aCC-BY-NC-ND 4.0 International license.

114 activation but may exhibit a chronic active BCR (13) and are sensitive to BTK inhibitors (14).
115 STAT3 activation mainly found in ABC-DLBCLs and is associated with poor survival (15).

116

117 Here, our results show that NF-κB activated B-cell lymphoma of the L.CD40 mouse model
118 exhibited an immune escape gene signature involving expression of PD-L1 and PD-L2, which
119 expression was co-clusterized with IL-10. Over-expression of PD-L1 expression not only
120 involved NF-κB activation by CD40 but also BTK and JAK/STAT signaling, the latter
121 probably being indirectly regulated via an autocrine loop with participation of IL-10 for
122 example. Indeed, PD-L1 expression could be down-regulated after treated with NF-κB,
123 JAK1/JAK2 and BTK inhibitors. Expression of PD-L1 was very likely to be associated to
124 tumor immune escape as demonstrated for numerous solid cancers such as melanoma of lung
125 cancers. Indeed, *in vivo* blockade of PD-L1 was able to rapidly repress expansion of these B-
126 cell lymphomas, with concomitant decrease in both B-cell proliferation and B-cell expression
127 of activation markers as well as an increase in T-cell activation. This clearly indicates that
128 therapies against the PD-L1/PD-1 axis may work in lymphomas as long as the tumor cells
129 express PD-L1. Our results also suggest that combination of immune therapy targeting the
130 PD-1/PD-L1 axis and TKI specific for the JAK/STAT or the BCR/BTK pathway could be of
131 interest, opening new perspective on the effect of these molecules on the reactivation of the
132 immune system.

133

134 **Material and Methods**

135 **Mouse models and *in vivo* and *ex vivo* treatments**

136 L.CD40 mice have been already described (5). Animals were housed at 21–23°C with a 12-h
137 light/dark cycle. All procedures were conducted under an approved protocol according to

bioRxiv preprint doi: https://doi.org/10.1101/502922; this version posted December 21, 2018. The copyright holder for this preprint (which was not certified by peer review) is the author/funder, who has granted bioRxiv a license to display the preprint in perpetuity. It is made available under aCC-BY-NC-ND 4.0 International license.

138 European guidelines for animal experimentation (French national authorization number: 87-
139 022 and French ethics committee registration number "CREEAL": 09-07-2012). For in vivo
140 PD-L1 treatment, L.CD40 mice were injected intraperitoneally every 4 days for three weeks
141 with 200 µg anti-PD-L1 antibody (clone 10F.9G2; Bio X cell; US). For ex vivo treatments,
142 splenocytes were cultured for 48 hours in complete RPMI medium (Eurobio) supplemented
143 with 10 % of FBS, 2mM of L-Glutamine, 1% of Na pyruvate, 100U/ml of penicillin and
144 100µg/ml of streptomycin (ThermoFisher Scientific) and with the following treatments: either
145 10 µM of PHA 408 or 1.5µM of Roxolitinib or 1µM of Ibrutinib.
146

147 **Flow cytometry**

148 Spleen from mice were collected and immune cells were filtered through a sterile nylon
149 membrane. Cell suspensions were stained at 4°C in FACS Buffer (PBS, 1% FBS, 2 mM
150 EDTA) with the following fluorescent-labelled antibodies: anti B220-BV421 (clone RA3-
151 6B2, 1/400), anti CD4-FITC (clone RM4-5, 1/2000), anti CD8a-APC (clone 53-6.7, 1/400),
152 anti CD62L-BV421 (clone MEL-14, 1/200), anti CD44-PE (clone IM7, 1/200), anti-PD-L1-
153 PE (clone 10F.9G2, 1/80), anti PD-1-PECy7 (clone 29F.1A12, 1/50), anti CD80-APC
154 (clone16-10A1, 1/2500) and anti CD86-FITC (clone GL-1, 1/600). Stained cells were
155 analyzed using a BD-Fortessa SORP flow cytometer (BD Bioscience; US). Results were
156 analyzed using Kaluza Flow Cytometry software 1.2 (Beckman Coulter; France).
157

158 **Proliferation**

159 For *in vivo* proliferation, mice were injected intraperitoneally with 2 mg BrdU (Sigma-
160 Aldrich, US), 18 hours before isolating cells. Splenocytes were stained for B220 and phases
161 of cell cycle were analyzed by measuring BrdU and Propidium Iodide (PI)-incorporation,
162 using the FITC-BrdU Flow Kit (BD Pharmingen; US).

bioRxiv preprint doi: https://doi.org/10.1101/502922; this version posted December 21, 2018. The copyright holder for this preprint (which was not certified by peer review) is the author/funder, who has granted bioRxiv a license to display the preprint in perpetuity. It is made available under aCC-BY-NC-ND 4.0 International license.

163

164 **Acknowledgments:** We thank Dr J Cook Moreau, UMR CNRS 7276, Limoges, France, for
165 English editing.

166

167 **Authorship Contributions**

168 C.V.F. performed, analyzed experiments and contributed to the writing. L.R. helped to
169 perform proliferation and flow cytometry experiments. U.Z.S. helped analyze the results and
170 contributed to the writing of the manuscript. J.F. and N.F. designed and directed the study,
171 contributed to the experiments, analyzed the results and wrote the manuscript.

172

173

bioRxiv preprint doi: https://doi.org/10.1101/502922; this version posted December 21, 2018. The copyright holder for this preprint (which was not certified by peer review) is the author/funder, who has granted bioRxiv a license to display the preprint in perpetuity. It is made available under aCC-BY-NC-ND 4.0 International license.

174 **References**

175 1. Durand-Panteix S, Farhat M, Youlyouz-Marfak I, Rouaud P, Ouk-Martin C, David A, et
176 al. B7-H1, which represses EBV-immortalized B cell killing by autologous T and NK
177 cells, is oppositely regulated by c-Myc and EBV latency III program at both mRNA and
178 secretory lysosome levels. J Immunol Baltim Md 1950. 2012;189:181–90.

179 2. Topalian SL, Drake CG, Pardoll DM. Immune checkpoint blockade: a common
180 denominator approach to cancer therapy. Cancer Cell. 2015;27:450–61.

181 3. Xu-Monette ZY, Zhou J, Young KH. PD-1 expression and clinical PD-1 blockade in B-
182 cell lymphomas. Blood. 2018;131:68–83.

183 4. Yu L, Li L, Medeiros LJ, Young KH. NF-κB signaling pathway and its potential as a
184 target for therapy in lymphoid neoplasms. Blood Rev. 2017;31:77–92.

185 5. Hömig-Hölzel C, Hojer C, Rastelli J, Casola S, Strobl LJ, Müller W, et al. Constitutive
186 CD40 signaling in B cells selectively activates the noncanonical NF-kappaB pathway
187 and promotes lymphomagenesis. J Exp Med. 2008;205:1317–29.

188 6. David A, Arnaud N, Fradet M, Lascaux H, Ouk-Martin C, Gachard N, et al. c-Myc
189 dysregulation is a co-transforming event for nuclear factor-κB activated B cells.
190 Haematologica. 2017;102:883–94.

191 7. Laurent C, Charmpi K, Gravelle P, Tosolini M, Franchet C, Ysebaert L, et al. Several
192 immune escape patterns in non-Hodgkin's lymphomas. Oncoimmunology.
193 2015;4:e1026530.

194 8. Koni PA, Bolduc A, Takezaki M, Ametani Y, Huang L, Lee JR, et al. Constitutively
195 CD40-activated B cells regulate CD8 T cell inflammatory response by IL-10 induction. J
196 Immunol Baltim Md 1950. 2013;190:3189–96.

197 9. Li L, Zhang J, Chen J, Xu-Monette ZY, Miao Y, Xiao M, et al. B-cell receptor-mediated
198 NFATc1 activation induces IL-10/STAT3/PD-L1 signaling in diffuse large B-cell
199 lymphoma. Blood. 2018;132:1805–17.

bioRxiv preprint doi: https://doi.org/10.1101/502922; this version posted December 21, 2018. The copyright holder for this preprint (which was not certified by peer review) is the author/funder, who has granted bioRxiv a license to display the preprint in perpetuity. It is made available under aCC-BY-NC-ND 4.0 International license.

200 10. Brunner C, Avots A, Kreth HW, Serfling E, Schuster V. Bruton's tyrosine kinase is
201 activated upon CD40 stimulation in human B lymphocytes. Immunobiology.
202 2002;206:432–40.

203 11. Zhang L, Gajewski TF, Kline J. PD-1/PD-L1 interactions inhibit antitumor immune
204 responses in a murine acute myeloid leukemia model. Blood. 2009;114:1545–52.

205 12. Deng L, Liang H, Burnette B, Beckett M, Darga T, Weichselbaum RR, et al. Irradiation
206 and anti-PD-L1 treatment synergistically promote antitumor immunity in mice. J Clin
207 Invest. 2014;124:687–95.

208 13. Davis RE, Ngo VN, Lenz G, Tolar P, Young RM, Romesser PB, et al. Chronic active B-
209 cell-receptor signalling in diffuse large B-cell lymphoma. Nature. 2010;463:88–92.

210 14. Wilson WH, Young RM, Schmitz R, Yang Y, Pittaluga S, Wright G, et al. Targeting B
211 cell receptor signaling with ibrutinib in diffuse large B cell lymphoma. Nat Med.
212 2015;21:922–6.

213 15. Huang X, Meng B, Iqbal J, Ding BB, Perry AM, Cao W, et al. Activation of the STAT3
214 signaling pathway is associated with poor survival in diffuse large B-cell lymphoma
215 treated with R-CHOP. J Clin Oncol Off J Am Soc Clin Oncol. 2013;31:4520–8.

216

217

bioRxiv preprint doi: https://doi.org/10.1101/502922; this version posted December 21, 2018. The copyright holder for this preprint (which was not certified by peer review) is the author/funder, who has granted bioRxiv a license to display the preprint in perpetuity. It is made available under aCC-BY-NC-ND 4.0 International license.

218 **Figure 1.** (A) Clustering of genes from the Immune Escape Gene Signature published by C
219 Laurent *et al.* for L.CD40 and WT mice. The specific cluster for L.CD40 mice is highlighted
220 in red. PD-L1 is pointed by the arrow. (B) Left panel, overlay example of PD-L1
221 monoparametric histograms gated on B220 B-cells. Right panel, flow cytometry Mean
222 Fluorescence Intensity (MFI) of PD-L1 on B-cells from 12 months old control CD19_Cre and
223 transgenic L.CD40 mice. Statistical significance was determined by unpaired t-test
224 (***P<0.001).
225

226 **Figure 2.** Flow cytometry Mean Fluorescence Intensity (MFI) of PD-L1 on B-cells after 48h
227 *in vitro* inhibitor treatments (PHA 408, Ruxolitinib and Ibrutinib). Statistical significance was
228 determined by unpaired t-test (***P<0.001; **P<0.01).
229

230 **Figure 3.** (A) Left panel, examples of whole spleens from Ctrl and αPD-L1 treated L.CD40
231 mice; middle panel, mean and standard deviation of spleen weight; right panel, absolute
232 numbers of spleen cells. For the PD-L1 treatment, L.CD40 mice were injected every 4 days
233 for three weeks with 200 µg anti-PD-L1 antibody in In VivoPure Dilution Buffer (clone
234 10F.9G2; Bio X cell; US). (B) Flow cytometry of spleen B220 B-cell absolute numbers in
235 Ctrl and αPD-L1 treated L.CD40 mice. (C) Flow cytometry of absolute numbers of spleen
236 B220 B-cells expressing CD80 and/or CD86 activation markers in L.CD40 after injection of
237 isotope control (Ctrl) or anti-PD-L1 (αPD-L1) antibody. (D) Mean and standard deviation of
238 flow cytometry percentages of BrdU positive B-cells after *in vivo* BrdU incorporation in Ctrl
239 and αPD-L1 treated L.CD40 mice. Mice were injected intraperitoneally with 2 mg BrdU, 18
240 hours before isolating cells. (E) May Grunwald staining of spleen imprints of Ctrl-L.CD40
241 (left panel) and αPD-L1-L.CD40 (right panel) mice. Statistical significance was determined
242 by unpaired t-test (**P<0.01; *P<0.05).

243 **Figure 4.** (A) Mean and standard deviation of flow cytometry percentages of activated $CD4^+$
244 and $CD8^+$ T cells expressing CD62L and CD44 activation markers in L.CD40 after injection

bioRxiv preprint doi: https://doi.org/10.1101/502922; this version posted December 21, 2018. The copyright holder for this preprint (which was not certified by peer review) is the author/funder, who has granted bioRxiv a license to display the preprint in perpetuity. It is made available under aCC-BY-NC-ND 4.0 International license.

245 of isotope control (Ctrl) or anti-PD-L1 (αPD-L1) antibody. (B) Flow cytometry Mean
246 Fluorescence Intensity (MFI) of PD1 on $CD4^+$ and $CD8^+$ T cells in Ctrl and αPD-L1 treated
247 L.CD40 mice. Statistical significance was determined by unpaired t-test (**P<0.01; *P<0.05).

Figure 1

A

LMP1CD40
WT

1

PTGS2
IL6
STAT3
VTCN1
IDO1
TIMP1
COL17A1
SOCS3
MYC
PDCD1
FOXP3
IL13
TNFRSF14
HAVCR2
TGFB1
PVR
LGALS1
GDF15
CCL2
VEGFA
PIM1
JAK2
PDCD1LG2
CSF1
MCL1
CD80
CD86
ENTPD1
IL10
ARG1
IL4
CD274
LAIR1
CD163
PTGS1
MRC1
IL6ST
CCL22
ICOS
CTLA4
LAG3
IDO2
HGF
MSR1
LGALS3
NT5E
BTLA

S7 S8 S5 S3 S11 S4 S6 S2 S10 S1 S9

+3SD +2SD +1SD mean -1SD -2SD -3SD

1

PIM1
JAK2
PDCD1LG2
CSF1
MCL1
CD80
CD86
ENTPD1
IL10
ARG1
IL4
CD274

B

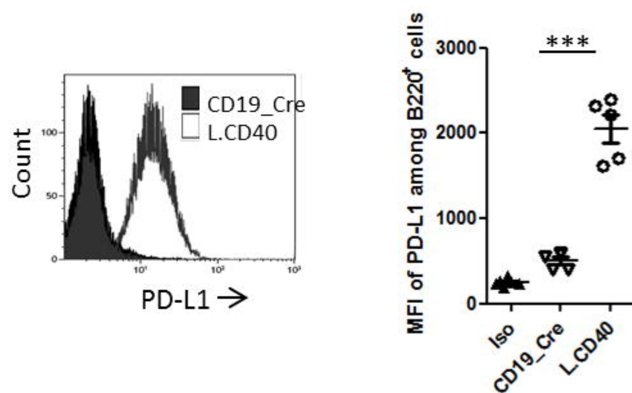

Figure 2

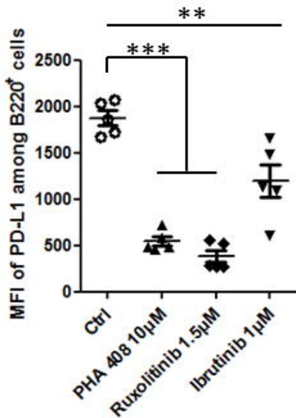

Figure 3

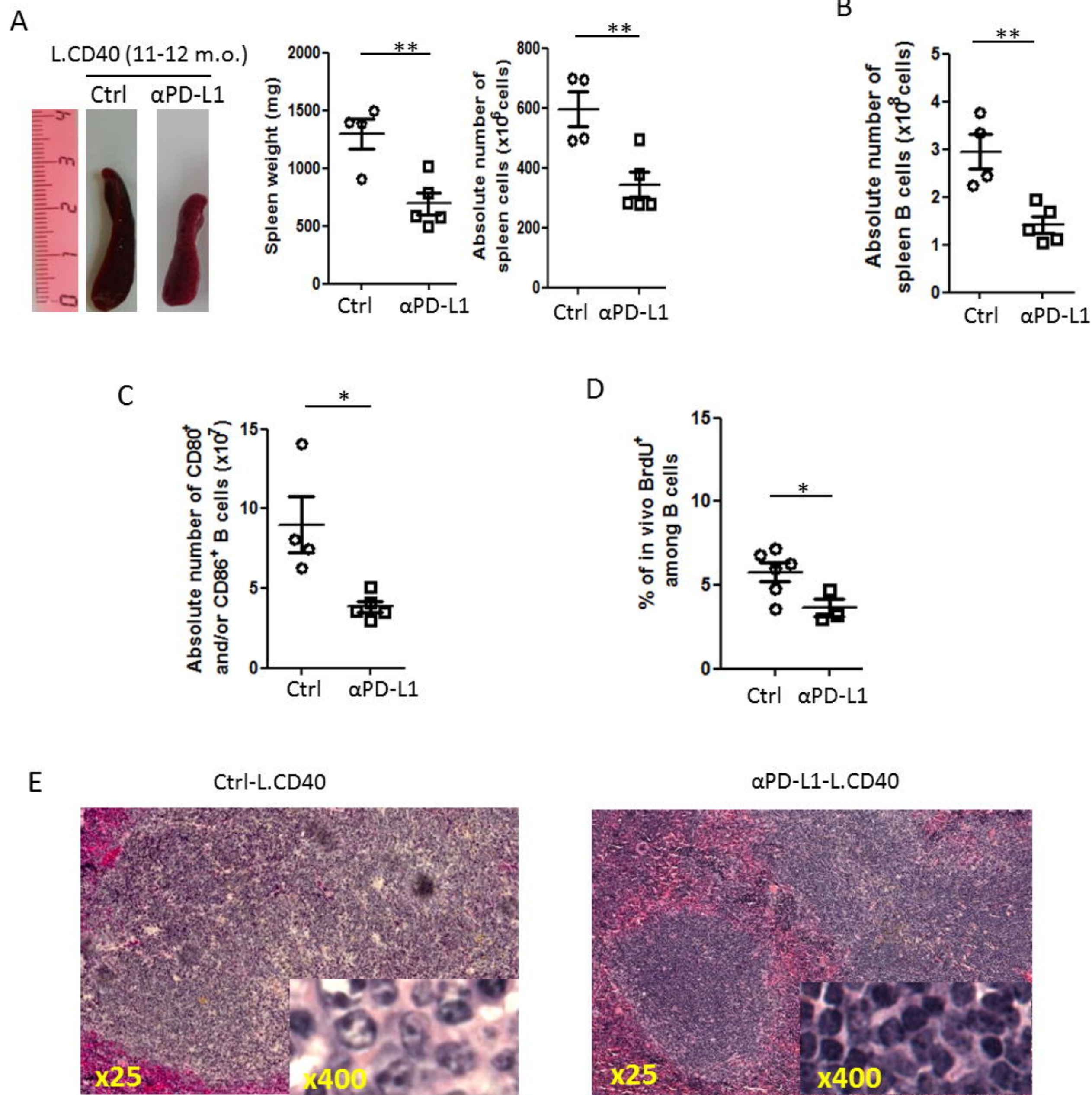

Figure 4